PHYSICAL REVIEW B VOLUME 48, NUMBER 19 15 NOVEMBER 1993-I

Morphology of monatomic step edges on vicinal Si(001)

H. J. W. Zandvliet*
Faculty of Applied Physics, University of Twente, P.O. Box 217, 7500 AE Enschede, The Netherlands

H. B. Elswijk
Philips Research Laboratories, P.O. Box 80 000, 5600 JA Eindhoven, The Netherlands
(Received 19 April 1993)

The roughness of monatomic *A*- and *B*-type step edges on 0.5° misoriented Si(001) has been analyzed on an atomic scale with scanning tunneling microscopy. On small length scales, measured along the step edge (<200 Å), one-dimensional random-walk behavior is observed for both types of step edges. For the rough *B*-type step edge we also found evidence for waviness of the edge. The period of this wave is about 100 dimer-row spacings ($\approx 750-800$ Å). The energetic step-step interaction and entropic repulsion, which both scale as $1/L^2$ (L is the average terrace length), are estimated to be about 0.03–0.06 and 0.2 meV per dimer-row spacing, respectively, for a 0.5° misoriented surface. These interactions are approximately three orders of magnitude smaller compared to the kink formation energies which are 0.1–0.2 eV. Despite the weak strength of energetic and entropic step-step interactions, these long-range interactions have a profound effect on the step-edge morphology, e.g., the distribution of terrace lengths and the long-range waving of the rough *B*-step edge.

I. INTRODUCTION

A real surface always shows steps due to the fact that it is virtually impossible to cut a crystal exactly along one of its low Miller indices planes. The number and height of step edges on a surface is a reflection of this macroscopic misorientation. Step edges play an important role in several surface processes. In epitaxial growth, for example, the presence and amount of step edges is very important for the growth mode that occurs on the surface. If the growth parameters are chosen such that the step edges act as sinks for incoming atoms the crystal will grow smoothly in what is called the step-flow mode. Another technical important example where step edges may play an important role is gas adsorption. Again the step edge can act as a preferential adsorption site. From a more fundamental point of view, the energetics and morphology of step edges are also challenging because there often exists a competition between strong short-range interactions, i.e., step-edge energies, and long-range energetic and entropic step-step interactions. Currently vicinal Si(001) surfaces are being studied intensively. The Si(001) surface reconstructs to form rows of dimerized atoms,[1] yielding a (2×1) unit cell. A slight misorientation with respect to the [001] direction in the [110] or $[\bar{1}10]$ direction (the [110] and $[\bar{1}10]$ directions correspond to the directions of the dimer rows) results in a vicinal Si(001) surface with monatomic steps. Proper cleaning of this surface[2] leads to a regular step distribution that reflects the macroscopic misorientation of the sample. Due to the symmetry of the silicon lattice (diamond structure), two types of steps can be distinguished on the Si(001) surface: steps running parallel and perpendicular to the dimer rows of the upper terrace. Steps parallel to the dimer rows of the upper terrace are straight (*A*-type steps[3]), whereas the others are ragged (*B*-type steps[3]), i.e., they exhibit a high density of thermally excited kinks.[4] For small miscut angles ($\vartheta<2°-3°$) the surface consists of two rotationally equivalent reconstruction domains, (2×1) and (1×2). The monatomic step edges are hence alternating rough and straight; see Figs. 1 and 2 for a schematic representation and a scanning tunneling microscopy (STM) image, respectively. It is interesting that at both large and small miscut angles the step edge morphology of Si(001) is determined by a competition of step-edge energies and step-step interactions (surface stress). For large ($\vartheta>2°-3°$) miscut angles biatomic steps have been found,[5–7] whereas for very small ($\vartheta<0.1°$) miscut angles wavy (sinusoidal) step edges coexist with straight steps.[8]

In this paper the step structure is interpreted in terms of a simple equilibrium statistical mechanical model. Kink formation energies, step-step interaction energies, entropic repulsion, the deviation-deviation correlation function of the step edges, and the distribution of terrace lengths are determined from room-temperature STM images. All of the main features in the deviation-deviation correlation function of the rough *B*-type step edge can be understood if a comparison with a wandering step edge trapped between two fixed walls is made and if entropic repulsion and waviness in the step edge are taken into account. The important aspect at which temperature thermal equilibrium of the step edges is achieved will be addressed with the aid of high temperature STM data of vicinal Si(001).

II. EXPERIMENT

Recently, Dijkkamp, van Loenen, and Elswijk[9] developed an ultrahigh vacuum (UHV) high-temperature scanning tunneling microscope (STM) for the observation

0163-1829/93/48(19)/14269(7)/$06.00

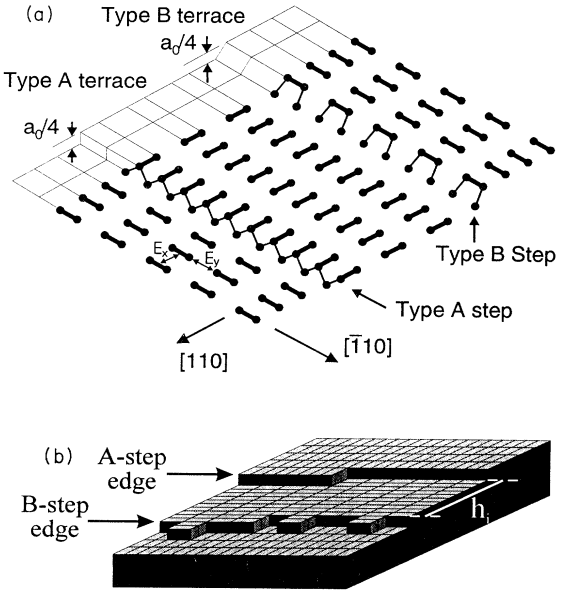

FIG. 1. (a) A ball and stick model of a tilted Si(001) surface with two nonequivalent monatomic steps [following the notation of Chadi (Ref. 3) these steps are denoted A- and B-type monatomic step edges, respectively]. The surface reconstructs to form rows of dimerized atoms. The dimer row directions are perpendicular (B-type) or parallel (A-type) to the step edge. $E_{x,y}$ refers to the nn interaction energies between dimers. (b) A schematic representation of the tilted Si(001) surface. Each rectangular block corresponds to a single dimer. The average terrace length is L and the monatomic step height ($a_0/4$) is 1.36 Å. Kink lengths are always multiples of a dimer row spacing (=7.7 Å). h_i is the length of a dimer row measured from an A-type step edge to the B-type step edge of the lower terrace.

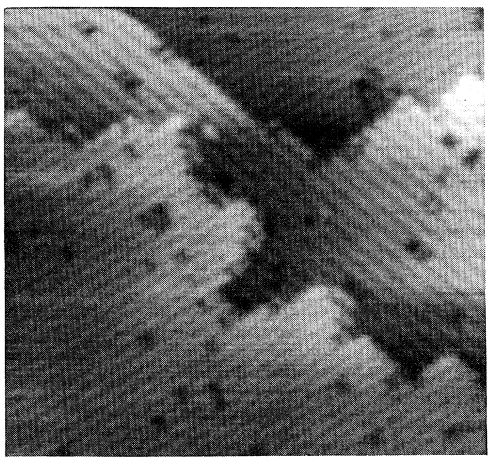

FIG. 2. An STM image (28×28 nm^2) of Si(001) 0.5° misoriented towards the [110] direction, obtained at −2-V sample bias and 0.5-nA tunneling current.

of surfaces at elevated temperatures. The general design of this instrument and its modifications are described elsewhere.[9] In general, both room temperature as well as high-temperature STM images were taken with a sample bias of −2 or −1.5 V and a typical tunneling current of 0.5–1 nA. The Si(001) samples were cut from commercially available wafers (Wacker, floating zone B-doped 8–12 Ω cm) and ultrasonically rinsed in ethanol before loading them into the vacuum system. The misorientation of the surface with respect to (001), as determined by x-ray diffraction, is about 0.5° in the [110] direction. Inside the UHV chamber, which has a base pressure below 1×10^{-10} Torr, the samples were heated resistively. The temperature was measured with an infrared pyrometer (calibrated against a NiCr-NiAl thermocouple) with an absolute accuracy of about 25 K. After outgassing the sample and holder for several hours the sample was thermally cleaned at 1500 K for several seconds. During cleaning the pressure was maintained below 1×10^{-9} Torr in order to avoid contamination of the sample surface. This procedure[2] results in a two-domain (2×1) reconstructed atomically clean Si(001) surface with an average terrace length of about 150 Å.

III. RESULTS AND DISCUSSION

A. Distribution of kinks and kink lengths: Roughness on the atomic scale

In Fig. 3 two typical large-area images (100×100 and 80×80 nm^2) of a 0.5° misoriented Si(001) surface, taken at room temperature, are shown. Figure 3(a) displays an atomically clean Si(001) surface whereas the surface in Fig. 3(b) has a slight Ni contamination (<1% of a monolayer), which gives rise to the characteristic dark dimer-defect rows. It is remarkable that the Ni contamination does not seem to have any effect on the roughness on an atomic scale of the monatomic step edges, i.e., the distribution of kinks and kink lengths. The step edges are alternating rough (B-type step edge) and straight (A-type step edge) and the average terrace length ($L\approx150$ Å) corresponds to about 20 dimer-row spacings (=7.7 Å). In order to analyze the roughness of the step edges on an atomic scale Swartzentruber *et al.*[10] originally introduced the idea to measure the distribution of kinks and kink lengths. By assuming that all the kinks are thermally excited, which is usually a good approximation for relatively rough step edges, they were able to extract the kink formation energies from these measured distributions. In a similar study we[11] have explicitly included the presence of forced kinks (caused by a misorientation of the step edge with respect to the [110] or [$\bar{1}$10] direction). Following the theory of Burton, Cabrera, and Frank,[4] we have used the thermodynamic relation

$$E_{x,y}=-k_bT\ln[n_{+1}n_{-1}/n_0^2]\ , \tag{1}$$

where $k_b=1.38\times10^{-23}$ J K^{-1} and T is the temperature in Kelvin. The symbol $n_{+r,-r}$ is used to denote the probability that there is a "jump" (+ kink) or a "drop" (− kink) of length r perpendicular to the step edge in the surface plane at a given position in the step edge [see Fig.

1(b)]. The probability of finding no kink at all at a certain position in the step edge is given by n_0. E_x refers to the nearest neighbor (nn) interaction energy between dimers in the same dimer row and E_y refers to the nn interaction energy between dimers in adjacent rows [see Fig. 1(a)]. Formula (1) can be understood as coming from a comparison of several different situations of the step edge, for example a n_{-1} and n_{+1} kink pair versus a straight step edge, that result in the same overall displacement of the step edge (the principle of detailed balancing[4]).

It is of major importance to note that no difference between forced kinks and thermally excited kinks has to be made; Eq. (1) is always valid. A large misorientation of a step edge corresponds to a large amount of forced kinks in one direction and, hence, to a low amount of thermally excited kinks in the opposite direction.

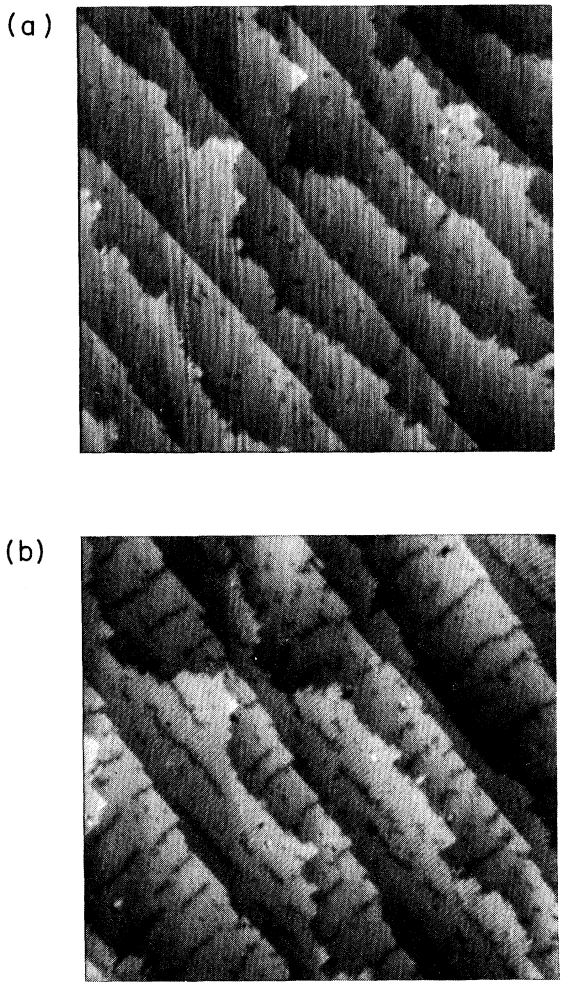

FIG. 3. (a) Large-area (100×100 nm^2) STM image of Si(001) 0.5° misoriented towards the [110] direction, obtained at -2-V sample bias and 0.5-nA tunneling current. (b) Large-area (80×80 nm^2) STM image of Si(001) slightly contaminated with Ni ($<1\%$ of a monolayer as determined with Rutherford backscattering spectroscopy). The Ni contamination gives rise to dimer-defect rows (visible as dark rows in the image) perpendicular to the dimer rows.

In Refs. 10 and 11 slightly extended models were used in order to interpret the data: in Ref. 10 a kink corner energy was introduced, whereas Ref. 11 included an isotropic next nn interaction energy. Nevertheless, if only kinks with length zero and one (n_0, n_1, and n_{+1}) are counted one can, using Eq. (1), determine the nn interaction energies. In this context it is very important to note that Eq. (1) doesn't alter if next nn interactions are taken into account.[11] In order to interpret the distributions of kinks and kink lengths in terms of nn interaction energies the temperature at which the roughness of the step edges is frozen in, T_f, should be known. In the room temperature images of vicinal Si(001) no changes were observed as a function of time, so T_f should certainly lie above 300 K. Scanning tunneling microscopy images of vicinal Si(001) recorded at 725 K (Ref. 12) (Fig. 4) show that the step edges change very slowly on a time scale of minutes. At 800 K the movement of the step edges becomes, as expected, significantly faster.[9] In our preparation method the samples were radiation quenched from 1500 K to about 500 K in a few seconds; therefore, the step structure observed at room temperature is typically frozen in at a temperature between about 725 and 825 K. As an estimate we have used a temperature of 775 K. This results in the following interaction energies: 0.38 eV between adjacent dimers within the same dimer row and 0.24 eV between sets of two dimers (the minimum kink length is $2a$) in adjacent dimer rows. If one breaks one bond along a step edge two kinks are created and thus the kink formation energies are 0.19 and 0.12 eV for a straight A-type and a rough B-type step edge, respectively.

In the next section the observed behavior of the step edges will be compared with an isolated step edge and a step edge trapped between two fixed walls. Particular beautiful theoretical work in this context has been published by Bartelt, Williams, and Einstein[13–18] as well as Gruber and Mullins[19] and Fisher and Fisher.[20] Below a brief outline of the relevant characteristics is given, for more theoretical details we refer to the foregoing references.

B. An isolated step edge: The random walker

We will start with the most simple case: an isolated step edge on a surface. The roughness of this step edge can be analyzed in more detail if we introduce the deviation-deviation correlation function of the step edge, $G(r)=\langle(h_0-h_r)^2\rangle$, where r is a distance measured parallel to the step edge (the timelike axis) and h_i is the deviation of the step edge in the direction perpendicular to it (see Fig. 1). Assuming equilibrium there is a random distribution of positive and negative kinks for an isolated step edge and hence $G(r)$ is proportional to r. Following Refs. 17 and 21 one can write

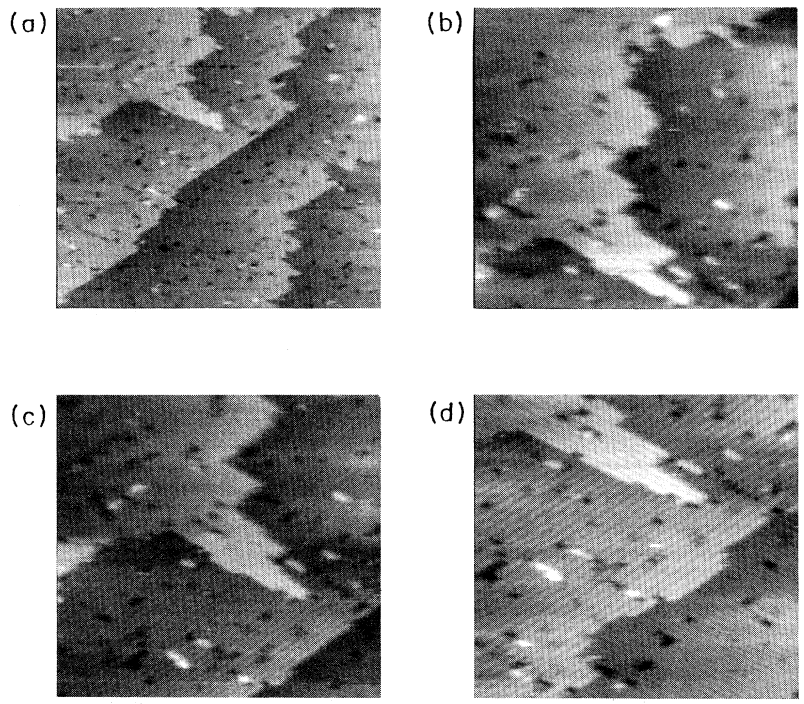

FIG. 4. (a) STM image of a vicinal Si(001) surface at 725 K (60×60 nm^2). (b)–(d) Three subsequent images (30×30 nm^2) of the protruding part of the step edge in (a). Time lapse between images (b) and (c) and (c) and (d) is 69 and 134 s, respectively. The tunneling current was 0.5 nA and the sample voltage was -1.5 V.

$$\langle (h_0-h_r)^2\rangle = \langle k^2\rangle r \tag{2}$$

with $\langle k^2\rangle$ the local mean square length of a kink.

$$\langle k^2\rangle = \sum k^2 n_k = \frac{\sum k^2 \exp(-E_k/k_bT)}{\sum \exp(-E_k/k_bT)}\ , \tag{3}$$

where n_k is the probability of a kink with length k. The summation $\sum$ runs over all possible k values. The value $\langle k^2\rangle$, which is the local mean square length of a kink or the diffusivity[17] of a kink, can immediately be extracted from the distribution of kinks and kink lengths as shown in Refs. 10 and 11. This analysis[10,11] results in a value of $\langle k^2\rangle = 1.7$ and $\langle k^2\rangle = 0.1$–0.2 for a B-type and an A-type step edge, respectively. In Fig. 5 a plot of $\langle (h_0-h_r)^2\rangle$ versus r for an A- as well as a B-type step edge of Si(001) is shown. $\langle (h_0-h_1)^2\rangle$ ($\equiv\langle k^2\rangle$), taken from Fig. 5, is 1.7 and 0.2 for a B-type and an A-type step edge, respectively. The overall slopes of the curves are about 2.4 and 0.1 for a B- and an A-type step edge, respectively. The experimental data show that for low r values ($r<20$) an almost exact random walk behavior is observed. Both step edges behave as if they were isolated. As shown in the inset of Fig. 5 this random walk behavior breaks down[21] for larger r values ($r>40$). The breakdown of the random-walk behavior, i.e., the decrease of the correlation function will be the subject of the next section.

C. A meandering step edge trapped between two fixed step edges

Consider now the more realistic case of a meandering step edge (B type) trapped between two straight step edges (A type) separated by a distance $2L$, L being the average spacing between two adjacent step edges. Repulsive interactions between the step edges will tend to limit the amount of meandering by making closely spaced steps unfavorable. Restricting step fluctuations, however, decreases the entropy term (S) and thus increases the free

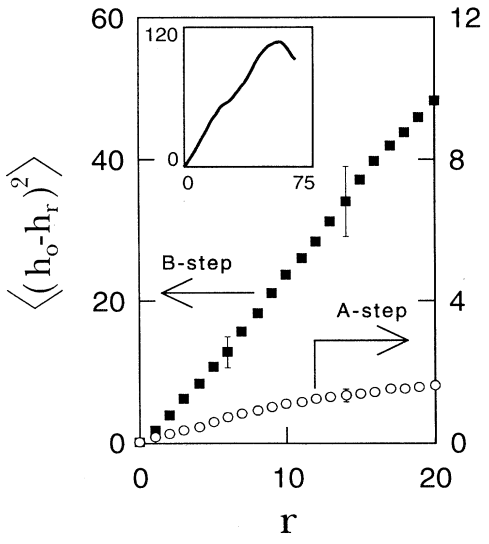

FIG. 5. Deviation-deviation correlation function $G(r)=\langle (h_0-h_r)^2\rangle$ of an A- and a B-type monatomic step edge vs the position difference r measured along the step edge. Typical error bars are indicated. Inset: $G(r)$ of a B-type step edge is shown for r values up to about $r=70$ dimer-row spacings. The units of r are dimer-row spacings.

energy, $F=U-TS$. The equilibrium distribution of the position of the B-type step edge is therefore peaked near the middle of the two fixed walls. To illustrate this we refer to the arguments given by Fisher and Fisher[20] for the case of a freely wandering wall between two fixed walls, with the only constraint that the steps are not allowed to cross. Each collision results in a decrease of the entropy with about $k_b \ln(2)$. The typical distance between collisions is given by $L^2/\langle k^2 \rangle$. Hence the free energy increase per dimer row spacing along the step edge is about $\langle k^2 \rangle k_b T \ln(2)/L^2$. Our experimental data, $\langle k^2 \rangle = 1.7$ and $L=20$, yields a free-energy increase of only $k_b T/340 \approx 0.2$ meV per dimer row spacing. Besides these entropic step-step interactions, however, it is also very likely that energetic step-step interactions may be present between the step edges.

Using elasticity theory Alerhand *et al.*[22] have shown that a crystal surface with degenerate phases and anisotropic surface stress tensor can lower its energy with respect to a uniform one-domain surface by forming an ordered domain configuration. The reduction in energy is due to a long-range elastic or strain relaxation of the surface that is driven by the difference in surface stress of the domains. Theoretical calculations[22,23] show that the surface stress tensor of Si(001) is indeed anisotropic: the surface is under tensile stress parallel to the surface dimers and under compressive stress in the direction perpendicular to the dimers. This leads to a strain energy relaxation energy per unit step length of

$$E_{\text{step-step}} = -C \ln(L/\pi a) , \tag{4}$$

where L is the width of the terraces, a ($=3.84$ Å) is the dimer-dimer spacing within a dimer row, and C is a constant. The potential $V(x,L)$ felt by a wandering step edge is in this case given by[14]

$$\begin{aligned} V(x,L) &= E_{\text{step-step}}(L+x) + E_{\text{step-step}}(L-x) \\ &\approx -2C \ln(L/\pi a) + Cx^2/L^2 . \end{aligned} \tag{5}$$

The last term in Eq. (5), C/L^2, refers to the step-step interaction per lattice spacing (the step-step displacement x is taken as ± 1 lattice spacing). In general, the problem of interacting noncrossing steps can be mapped onto the problem of interacting, spinless fermions.[24,25] The problem of finding the step distance distribution $P(x)$ is hence simply the solution of a 1D Schrödinger equation. Assuming no energetic step-step interactions gives $P(x,L) = (1/L)\cos^2(\pi x/2L)$, whereas for the case of energetic step-step interactions

$$P(x,L) = \frac{1}{w\sqrt{(2\pi)}} \exp(-x^2/2w^2)$$

will be found,[14] in which w is the width of the Gaussian

$$w(T,L) = \left[\frac{k_b T \langle k^2 \rangle L^2}{8C} \right]^{1/4} . \tag{6}$$

Figure 6 shows the distribution of terrace lengths (h_i), determined from several STM images of adjacent areas.

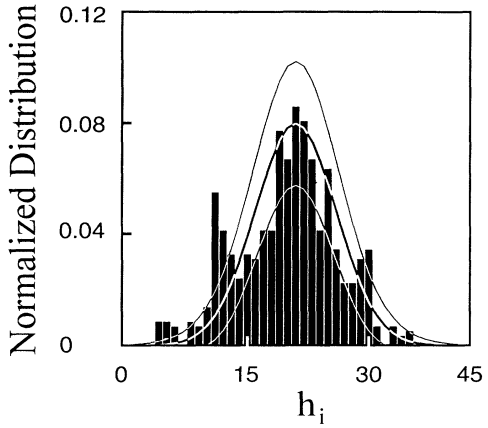

FIG. 6. Terrace width distribution (distance h_i, measured from an A-type step edge to a B-type step edge of the lower terrace) for a 0.5° off Si(001) surface. The average terrace length corresponds to approximately 20 dimer-row spacings (L_{average}). Bold line: Gaussian centered around $h_i = 21$, the width is 5. Normal lines: Gaussian $\pm 2\sigma$, σ is the calculated standard deviation for a Gaussian data set with the exact size of our experimental data set. The units of h_i are dimer-row spacings.

If the weak but significant shoulders, located symmetrically around the main peak, are neglected the data can be fitted with a Gaussian of width $w \approx 4-5$ and hence a C value of about 10–25 meV/$2a$ ($2a \approx 7.7$ Å is the dimer-row spacing) is obtained. Hence C/L^2, the energetic step-step interaction, has a value of about 0.03–0.06 meV/$2a$. Bearing in mind that the entropic step-step repulsion is about 0.2 meV/$2a$ we must conclude that both interactions are of the same order of magnitude. In spite of the weak strength of these long-range interactions compared to the kink formation energies, they are responsible for the very peaked shape of the terrace width distribution. A recent paper by de Miguel *et al.*[26] also shows evidence for a peaked distribution of terrace lengths of 0.5° misoriented Si(001). Their distribution is comparable with ours although the shoulders in their image are much weaker. At the moment we still cannot explain the weak shoulders in our distribution of the terrace widths. On the basis of the curves plotted in Fig. 6 we believe, however, that the weak shoulders we observed are not due to statistical noise.

The inset of Fig. 5 displays an experimental observation which is in favor of the existence of step-edge waviness in the rough B-type step edge at a miscut angle of 0.5°. Moreover, a decrease of the deviation-deviation correlation function can clearly be observed. For the straight A-type step edge, however, we did not find any indication of the existence of step-edge waviness. A decrease of the deviation-deviation correlation function implies step-edge waviness.[21] To illustrate the foregoing interpretation we have superimposed a sinus wave,[8] $A \sin(2\pi r/\lambda)$, on a meandering step edge trapped between two fixed walls. The deviation-deviation correlation function, $\langle (h_0 - h_r)^2 \rangle$, of a wandering step edge between two fixed walls is given in Ref. 17. If the sinus wave is also included we find

$$\langle (h_0-h_r)^2\rangle = (2/3-4/\pi^2)L^2 - \frac{2048L^2}{\pi^4} \times \sum_{p=1}^{\infty} \frac{p^2}{(4p^2-1)^4} e^{-r/\xi} + A^2[1-\cos(2\pi r/\lambda)]$$

with

$$\xi = \frac{8L^2}{(4p^2-1)\pi^2\langle k^2\rangle} . \quad (7a)$$

For $r \ll (2/3-4/\pi^2)L^2/\langle k^2\rangle$, Eq. (7a) reduces to

$$\langle (h_0-h_r)^2\rangle = \langle k^2\rangle r + A^2[1-\cos(2\pi r/\lambda)] , \quad (7b)$$

and for $r \gg (2/3-4/\pi^2)L^2/\langle k^2\rangle$ Eq. (7a) approaches

$$\langle (h_0-h_r)^2\rangle = (2/3-4/\pi^2)L^2 + A^2[1-\cos(2\pi r/\lambda)] . \quad (7c)$$

For small r values ($r \ll \lambda$) the linear term in Eq. (7b) dominates, whereas for $r > \lambda/2$ a decrease of the deviation-deviation correlation function will be found. The slight increase of the slope of the curve of the B-type step edge from Fig. 5 at small r values is also in agreement with Eqs. (7a) and (7b). Taking $\langle k^2\rangle = 1.7$, $\lambda = 100$, $L = 20$, and $A = 5$ (A and λ are the only free parameters) the inset of Fig. 5 can be fitted very nicely (see Fig. 7). Although Eq. (7a) is not an excellent fit (see Fig. 7) it contains all the main features described above including a correct value for the maximum of $\langle (h_0-h_r)^2\rangle$ at $r \approx \lambda/2$. Very recently, Tromp and Reuter[8] found step-edge waviness for Si(001) surfaces which are misoriented less than 0.1°. This wavy phase is stabilized by a reduction of surface-stress-induced strain energy and coexists at a miscut angle of 0.1° with a phase of straight step edges. The period of the waviness for very flat Si(001) is about 1–2 μm and cannot be immediately compared with the period of about 750–800 Å we found for 0.5° off Si(001). Despite the much smaller period of the waviness (and amplitude) we may speculate that the waviness we found in the rough B-type step edge has also its origin in long-range step-step interaction. Following Tersoff and Pehlke[8] we can give a crude estimate for the period of the waviness (for the sake of simplicity we have taken a rectangular wave with period λ) in the rough B-type step edge. The step-edge energy of equally spaced A-type step edges is given by $E_{\text{step}} = E_{sa} - C \ln(L/\pi a)$, where E_{sa} is the step-edge formation energy of a single A-type step [=85 meV/2a (Ref. 11), if next nn interactions are included] and the definition of C is given by Eq. (4). The energy per area, E_{step}/L, has a minimum at the step separation

$$L^* = \pi a \exp(1 + E_{sa}/C) , \quad (8)$$

taking $C = 25-10$ meV/2a, gives $L^* \approx 250a - 4.10^4 a$ ($= 125 - 2.10^4$ dimer-row spacings). This strong variation of L^* is due to its exponential dependence on the ratio E_{sa}/C. The lower limit of L^* is in reasonable agreement with our own experiments, whereas the period observed by Tromp and Reuter (1–2 μm) is of the order of the upper bound of L^*. In contrast to the observation that at small miscut angle both types of step edges exhibit waviness, we only found evidence for waviness in the rough B-step edge and not in the straight A-type step edge. This last result is in agreement with microprobe diffraction studies performed by Tong and Bennett.[27] Due to the limited field of view of our STM we are not able to say anything about the morphology of the step edges which go beyond a length scale of 0.2 μm.

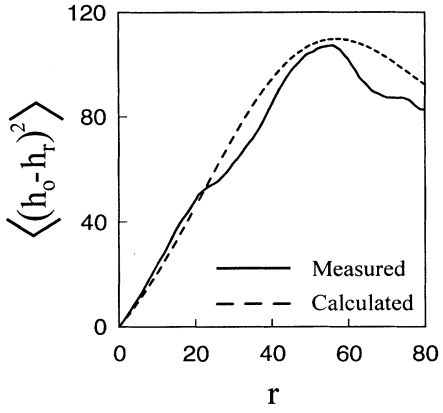

FIG. 7. Solid line: measured deviation-deviation correlation function of the B-type step edge. Dotted line: calculated deviation-deviation correlation function of the B-type step edge using Eq. (7a) with $L = 20$, $\lambda = 100$, $A = 5$, and $\langle k^2\rangle = 1.7$.

Finally, we want to note that on the basis of the STM images we have analyzed so far and which were all taken from the same area of the surface, we cannot rule out the possibility of coexistence of regions with wavy and straight step edges for 0.5° misoriented Si(001).

IV. CONCLUSIONS

We have analyzed the roughness of monatomic step edges on 0.5° misoriented Si(001) from an atomic scale up to a scale of about 0.1 μm. Besides kink formation energies also energetic and entropic step-step interactions are extracted from room temperature STM images. Both energetic and entropic step-step interactions scale as $1/L^2$ and are for our 0.5° misoriented samples about three orders of magnitude smaller compared to the kink formation energies which are in the range 0.1–0.2 eV. It is remarkable that these relatively weak step-step interactions have such a profound effect on the morphology of the step edges. Two examples are given in this paper: the peaked terrace width distribution and the waviness in the rough B-type step edge. We found, however, no evidence for waviness in the straight A-type step edges.

Note added. After the submission of this work a paper by Swartzentruber *et al.* [Phys. Rev. B **47**, 13 432 (1993)] came to our attention. These authors also determined the strength of the step-step interactions from the distribution of terrace lengths. Their results are in very good agreement with ours.

ACKNOWLEDGMENTS

H.J.W.Z. thanks Philips Research Laboratories, especially Dr. H. van Houten, for continuous support during the course of this work. The authors thank Dr. E. J. van Loenen, Dr. D. Dijkkamp, Dr. H. Wormeester, Dr. E. G. Keim, and D. J. Wentink for many valuable discussions and suggestions. D. J. Wentink is also gratefully acknowledged for preparing Figs. 1, 5, 6, and 7 of this paper.

---

*Electronic address: zvt@eltn.utwente.nl

[1]R. E. Schlier and H. E. Farnsworth, J. Chem. Phys. **30**, 917 (1959).

[2]D. Dijkkamp, A. J. Hoeven, E. J. van Loenen, J. M. Lenssinck, and J. Dieleman, Appl. Phys. Lett. **56**, 39 (1990).

[3]D. J. Chadi, Phys. Rev. Lett. **59**, 1691 (1987).

[4]W. K. Burton, N. Cabrera, and F. C. Frank, Philos. Trans. R. Soc. London. Ser. A **243**, 299 (1951).

[5]O. L. Alerhand, A. N. Berker, J. D. Joannopoulos, D. Vanderbilt, R. J. Hamers, and J. E. Demuth, Phys. Rev. Lett. **64**, 2406 (1990).

[6]T. W. Poon, S. Yip, P. S. Ho, and F. F. Abraham, Phys. Rev. Lett. **65**, 2161 (1990).

[7]E. Pehlke and J. Tersoff, Phys. Rev. Lett. **67**, 465 (1991); **67**, 1290 (1991).

[8]R. M. Tromp and M. C. Reuter, Phys. Rev. Lett. **68**, 820 (1992); J. Tersoff and E. Pehlke, *ibid.* **68**, 816 (1992).

[9]D. Dijkkamp, E. J. van Loenen, and H. B. Elswijk, in *Ordering at Surfaces and Interfaces,* edited by A. Yoshimori, T. Shinjo, and H. Watanabe, Springer Series in Material Science Vol. 17 (Springer-Verlag, Heidelberg, 1992), p. 85.

[10]B. S. Swartzentruber, Y.-W. Mo, R. Kariotis, M. G. Lagally, and M. B. Webb, Phys. Rev. Lett. **65**, 1913 (1990).

[11]H. J. W. Zandvliet, H. B. Elswijk, E. J. van Loenen, and D. Dijkkamp, Phys. Rev. B **45**, 5965 (1992).

[12]H. J. W. Zandvliet, H. B. Elswijk, and E. J. van Loenen, Surf. Sci. **272**, 264 (1992).

[13]E. D. Williams and N. C. Bartelt, Science **251**, 393 (1991).

[14]N. C. Bartelt, T. L. Einstein, and E. D. Williams, Surf. Sci. Lett. **240**, L591 (1990).

[15]N. C. Bartelt, T. L. Einstein, and E. D. Williams, Surf. Sci. **244**, 149 (1991).

[16]N. C. Bartelt, J. L. Goldberg, T. L. Einstein, and E. D. Williams, Surf. Sci. **273**, 252 (1992).

[17]N. C. Bartelt, T. L. Einstein, and E. D. Williams, Surf. Sci. **276**, 308 (1992).

[18]B. Joós, T. L. Einstein, and N. C. Bartelt, Phys. Rev. B **43**, 8153 (1991).

[19]E. E. Gruber and W. W. Mullins, J. Phys. Chem. Solids **28**, 875 (1967).

[20]M. E. Fisher and D. S. Fisher, Phys. Rev. B **25**, 3192 (1982).

[21]H. J. W. Zandvliet, H. Wormeester, D. J. Wentink, A. van Silfhout, and H. B. Elswijk, Phys. Rev. Lett. **70**, 2122 (1993).

[22]O. L. Alerhand, D. Vanderbilt, R. D. Meade, and J. D. Joannopoulos, Phys. Rev. Lett. **61**, 1973 (1988).

[23]M. C. Payne, N. Roberts, R. J. Needs, M. Needels, and J. D. Joannopoulos, Surf. Sci. **211**, 1 (1989).

[24]C. Jayaprakash, Craig Rottmann, and W. F. Saam, Phys. Rev. B **30**, 6549 (1984); D. E. Wolf and J. Villain, *ibid.* **41**, 2434 (1990).

[25]J. Frohn, M. Giessen, M. Poensgen, J. F. Wolf, and H. Ibach, Phys. Rev. Lett. **67**, 3543 (1991).

[26]J. J. de Miguel, C. E. Aumann, S. G. Jaloviar, R. Kariotis, and M. G. Lagally, Phys. Rev. B **46**, 10257 (1992).

[27]X. Tong and P. A. Bennett, Phys. Rev. Lett. **67**, 101 (1991).

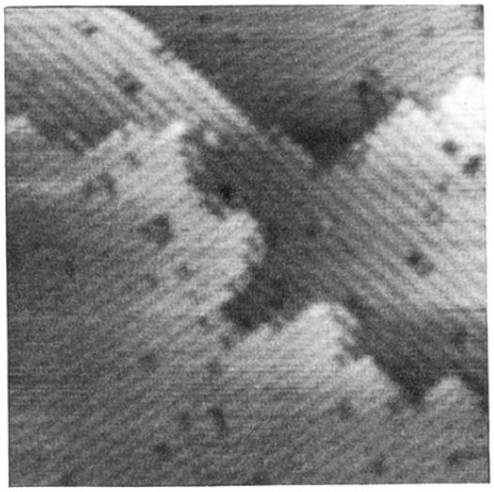

FIG. 2. An STM image (28×28 nm^2) of Si(001) 0.5° misoriented towards the [110] direction, obtained at -2-V sample bias and 0.5-nA tunneling current.

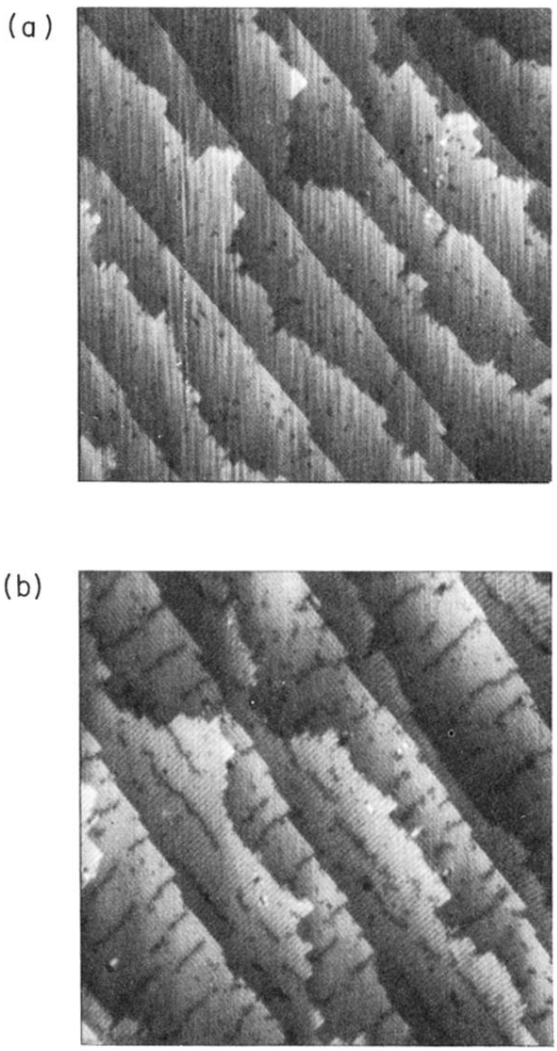

FIG. 3. (a) Large-area (100×100 nm^2) STM image of Si(001) 0.5° misoriented towards the [110] direction, obtained at -2-V sample bias and 0.5-nA tunneling current. (b) Large-area (80×80 nm^2) STM image of Si(001) slightly contaminated with Ni ($<1\%$ of a monolayer as determined with Rutherford backscattering spectroscopy). The Ni contamination gives rise to dimer-defect rows (visible as dark rows in the image) perpendicular to the dimer rows.

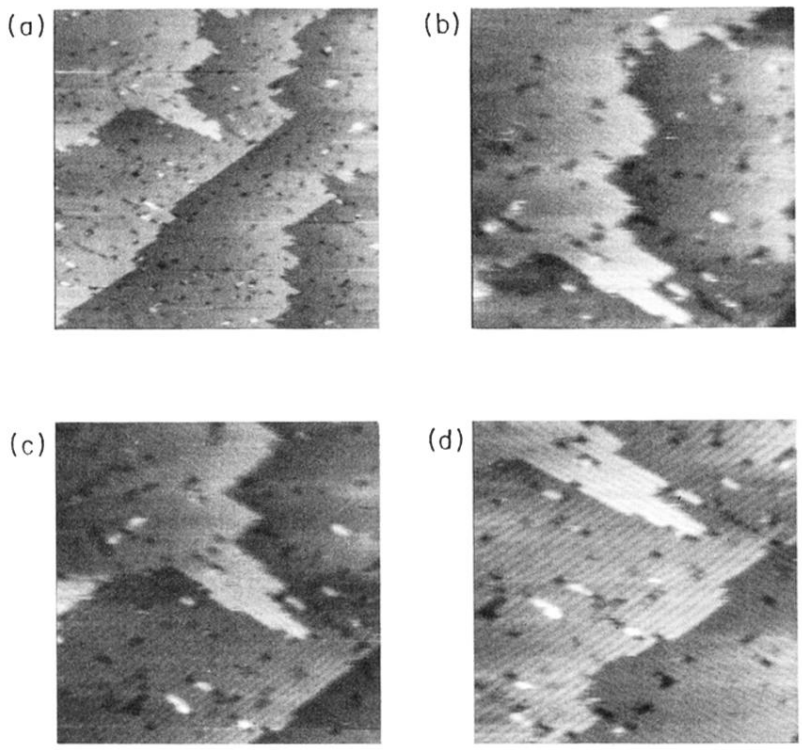

FIG. 4. (a) STM image of a vicinal Si(001) surface at 725 K (60×60 nm^2). (b)–(d) Three subsequent images (30×30 nm^2) of the protruding part of the step edge in (a). Time lapse between images (b) and (c) and (c) and (d) is 69 and 134 s, respectively. The tunneling current was 0.5 nA and the sample voltage was -1.5 V.